RECONSTRUCTING 3D BUILDINGS FROM LIDAR DATA

Ahmed F. Elaksher and James S. Bethel

School of Civil Engineering, Purdue University, 1284 Civil Engineering Building, West Lafayette, IN 47906, USA
elaksher@ecn.purdue.edu bethel@ecn.purdue.edu

ABSTRACT

Accurate 3D surface models in urban areas are essential for a variety of applications, such as visualization, GIS, and mobile communications. Since manual surface reconstruction is very costly and time consuming, the development of automated algorithms is of great importance. On the other hand LIDAR data is a relatively new technology for obtaining Digital Surface Models (DSM) of the earth's surface. It is a fast method for sampling the earth's surface with a high density and high point accuracy. In this paper a new approach for building extraction from LIDAR data is presented. The approach utilizes the geometric properties of urban buildings for the reconstruction of the building wire-frames from the LIDAR data. We start by finding the candidate building points that are used to populate a plane parameter space. After filling the plane parameter space, we find the planes that can represent the building roof surfaces. Roof regions are then extracted and the plane parameters are refined using a robust estimation technique and the geometric constraint between adjacent roof facets. The region boundaries are extracted and used to form the building wire-frames. The algorithm is tested on two buildings from a locally acquired LIDAR data sets. The test results show some success in extracting urban area buildings.

1. INTRODUCTION

LIDAR (Light Detection and Ranging) data is dense, with high accuracy, but one still needs to extract higher-level features from it. Building representations are needed in cartographic analysis, urban planning, and visualization. Although one pair of images, using photogrammetry, is adequate to find the 3D position of two corresponding and visible image features; it is not sufficient to extract the entire building due to hidden parts of the building that are not seen in the image pair. Building extraction can be done using multiple images to avoid this deficiency. On the other hand buildings can also be extracted directly from digital surface models as those produced by LIDAR.

The development of airborne laser scanning goes back to the 1970s (Jennifer and Jeff 1999). By emitting a laser pulse and precisely measuring the return time to the source the range can be calculated using the value for the speed of light. In the late-80s kinematic GPS provided the necessary centimeter level positioning accuracy required for high performance LIDAR. The systems required ultra-accurate clocks for timing the return, and Inertial Measurement Units (IMU) for capturing the orientation of the scanner (Wehr and Lohr 1999). Figure 1 shows the LIDAR system components. The system is an active system, so the data can be gathered during the day or night. LIDAR data pre-processing is composed of two efforts. First, the data must be filtered for noise, differentially corrected, and assembled into flight lines by return layer. Second, the LIDAR data may undergo further analysis to derive the final grided DEM products using interpolation.

In this paper a fully automated technique to extract urban building wire-frames from LIDAR data is presented. A minimum filter is used to find the candidate building points in the area. Plane regions are then extracted from the candidate building points. Planes with simple shapes are selected and adjacency conditions are enforced. Points and lines that define the resulting wire-frames are designated to form an arc-node structure for its representation. Results are shown for two buildings. Although the approach shows some success, the data density limits the extent of capturing small details.

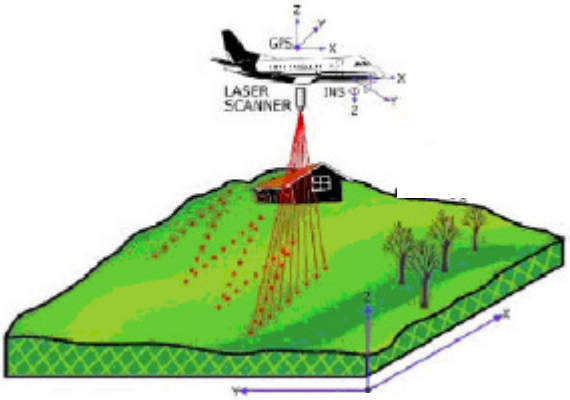

Figure 1. LIDAR System Components (Renslow, 2001)

2. OVERVIEW OF CURRENT BUILDING EXTRACTION SYSTEMS

In Morgan and Tempeli (2000) DEM production from laser data is presented. The procedure starts by re-sampling the irregular elevation points obtained by laser scanning into a regular grid. The core part of the building detection is based on a morphological filter for distinguishing between terrain and non-terrain segments. Aiming at a vector representation of buildings, the roof faces are obtained by further segmentation of the building segments into sub-segments. The 3D geometrical properties of each face are obtained based on plane fitting using the least squares technique. The reconstruction part of the procedure is based on the adjacency among the roof faces. Primitive extraction and face intersections are used for roof reconstruction. Prior knowledge about the buildings and terrain is needed for both the detection and extraction processes.

In Seresht and Azizi (2000) the authors describe a strategy for automatic building extraction from aerial imagery and digital elevation models. The first step is a coarse recognition of building regions from DEM. Then some filters are applied on the selected regions based on their shape, size and content to enhance the detectability of the buildings. Further

recognition is then achieved based on image features that include points, edges, and lines. Selection of type and level of feature extraction is related to the desired accuracy and method of reconstruction. Also straight lines are usually a basic characteristic of conventional buildings with regular edges. Buildings are then reconstructed from the listed features.

In Wang (2000) Building Extraction from a high quality terrain surface is presented. The approach takes terrain surface data as input and goes through edge detection, edge classification, building point extraction, TIN model generation, and building reconstruction to extract and reconstruct buildings and building related information. For building detection, the presented algorithm detects edges from the surface data and classifies edges to distinguish building edges from other edges based on their geometry and shapes, including orthogonality, parallelism, circularity and symmetry. The classified building edges are then used as boundaries to extract building points and TIN models are generated with the extracted points. Each building has its own TIN model and its surfaces are derived from the TIN model.

In Zhao and Trinder (2000) building extraction from aerial images and DEM is presented. In this research, a building is modeled as a polyhedron, comprising planes that are connected to form a solid volume. The intersections of adjacent planes are straight lines. The polyhedron has a set of attributes describing its geometry, radiometry, texture, topology, and context. From this model in order to address the complexity of the problem, the system consists of three parts: building detection, building segment extraction, and 3D segment matching and building modeling. The detection process starts with segmentation of the DSM (Digital Surface Model) to derive regions of interest (ROI) that have high expectation of representing individual buildings. Texture and shadow information are extracted and used to refine and verify the ROI. Buildings are constructed in a bottom-up approach. Primitive linear features are first derived, and relevant building polygons are extracted by grouping and filtering these primitive features within individual building regions. 3D lines are then generated by feature matching of these segments. Based on the matched lines, buildings are reconstructed by piecewise plane formation and plane intersection.

3. EXTRACTING ROOF REGIONS

In this section the process of extracting the building roof regions is described. The first step is to find the building candidate points; this is done by convolving the LIDAR DEM with a minimum filter. The second step is to extract the roof planes from the LIDAR DEM. This is done by voting in a plane parameter space and finding the cells in the parameter space with large numbers of points. LIDAR DEM points are then classified based on the plane to which they contribute. A region-growing algorithm is then used to complete the roof region extraction.

A minimum filter is first used for the process of finding building candidate points. First the DEM is convolved with the filter. The second step is to calculate the difference in the elevations between the original DEM and its filtered version. The differences in the elevations are used to select the candidate building points. All points with a height of 5.0 meters or more above the surrounding terrain are classified as building points. Figure 2-a,b,c, and d show the LIDAR DEMs and the candidate building points for two buildings.

The next step is to vote in the plane parameter space. The plane equation is presented by Equation (1). The two parameters a, b, represent two slopes in the X and Y directions and the parameter c is an offset parameter. In this research, the DEM grid was oriented nearly parallel with the building orientation and only one of the slopes, at most, was significantly different from zero. This allowed reduction of parametric space from 3 to 2. We used a 2D parameter space for the plane detection step after defining the main direction of the building, i.e. one of the two slope parameters is pre-selected to be zero.

$$Z = aX + bY + c$$

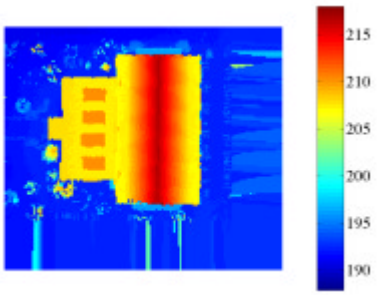

Figure 2-a. The Elevation Shaded LIDAR DEM (Building 1)

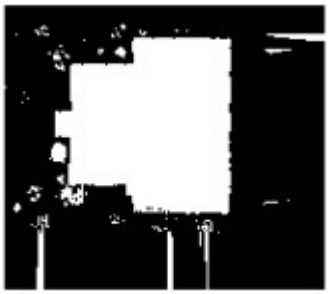

Figure 2-b. The Candidate Building Points (Building 1)

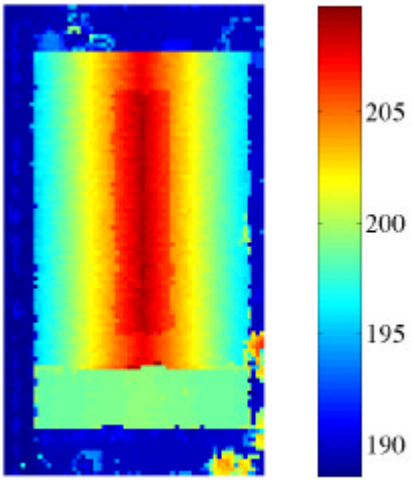

Figure 2-c. The Elevation Shaded LIDAR DEM (Building 2)

Figure 2-d. The Candidate Building Points (Building 2)

For each building candidate point a window is constructed around the point. All candidate points in the window are used to fit a plane using Equation (1). For each candidate point nine positions were tried and the position with the minimum residual was selected. This helps to include corner points and edge points, where the candidate point is either in the window corner or on its edge. A linear least squares estimation approach (Mikhail, *et. al.* 2001) is used to find the plane parameters at each point. If a statistic representing misclosure is small, the plane parameters at this point are used to vote in the 2D parameter space. Figure 3-a and b show the parameter space for the two buildings previously illustrated.

The window size and the parameter space cell size are based on the quality of the LIDAR data and the building characteristics. Poor quality data forces the cell size to be large in order to compensate for variation in the evaluated parameters of different points in the same plane. The relationship between points and their associated parameter cell is preserved for later use. The approach is similar to that used in Davies *et. al.* (1988) to extract straight lines.

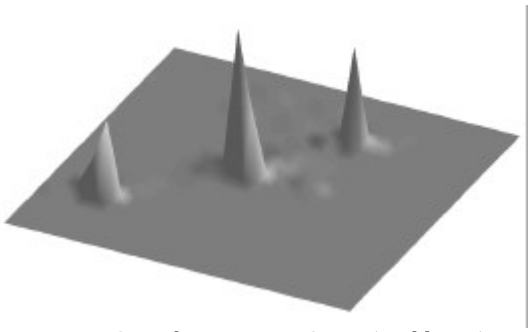

Figure 3-a. The Parameter Space (Building 1)

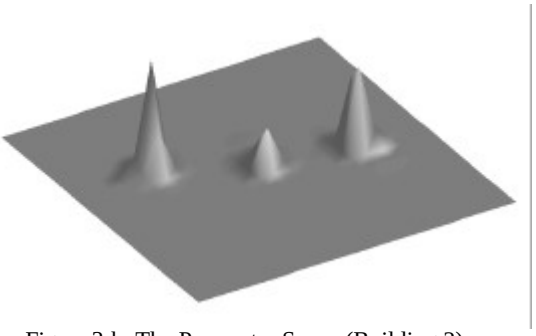

Figure 3-b. The Parameter Space (Building 2)

The parameter space is then searched to find peak cells. Cells with a high number of contributing points are identified and used as the building planes. The minimum number of points in the cell to be used as the threshold varies depending on the data quality, building size, and DEM resolution. Each cell is then given an identification number to identify this plane. Points that contribute to a certain plane are then categorized using their plane identification number. Plane regions are then extracted using the identification number. Each point in the DEM has its plane identification number. We used a region-growing algorithm (Jain, 1989) to connect points with the same identification number. Regions with small areas are then eliminated, while other regions are kept as the building roof regions. Holes in the roof regions are then filled. Figure 4-a and b show the extracted roof regions. The roof regions are used to extract the roof boundaries in the next section.

Figure 4-a. Extracted Roof Regions (Building 1)

Figure 4-b. Extracted Roof Regions (Building 2)

4. LIDAR DEM REFINEMENT

For each plane, the contributing points are used to adjust the plane parameters. The L1 norm (Marshall, 1998) is used in this step to update the plane parameters. L1 norm minimization is a robust estimation technique that has the ability to perform well in the presence of outliers. The updated parameters serve as the plane parameters at this stage. The elevations of all points that contribute to a certain plane are taken as observations, while the unknowns are the plane parameters.

The next step is to apply the geometric constraints of the building roofs. The first constraint is the horizontal plane constraint. The plane parameters are checked to find if any plane has small slope values, i.e. the values of the parameters ***a*** and ***b*** are negligibly different from zero. In this case the plane is assumed horizontal. The second constraint is the symmetric constraint. Each two adjacent planes are checked to find if they satisfy a slope symmetry condition, as one would expect in a conventional gabled roof. The previous constraints are used to update the plane parameters. The mathematical description for horizontal planes is shown in Equation (2). The complete mathematical description that is used to find the parameters of two symmetric planes is shown in Equation (3).

$$\begin{aligned} &Z_{n\times 1} - aX_{n\times 1} - bY_{n\times 1} - c = 0 \\ &\quad a = 0 \quad AND \quad b = 0 \end{aligned} \tag{2}$$

Where n is the number of points in the region.

$$\begin{aligned} &Z_{n\times 1} - a_i X_{n\times 1} - b_i Y_{n\times 1} - c_i = 0 \\ &Z_{m\times 1} - a_j X_{m\times 1} - b_j Y_{m\times 1} - c_j = 0 \\ &a_i + a_j = 0 \quad OR \quad b_i + b_j = 0 \end{aligned} \tag{3}$$

Where n is the number of points in region (i), m is the number of points in region (j). The overdetermined system is solved by least squares. The adjusted plane parameters are then used to refine the LIDAR DEM points. Each point elevation is refined based on the new plane parameters. Figure 5 and Figure 6 show the LIDAR DEM before and after the refinement.

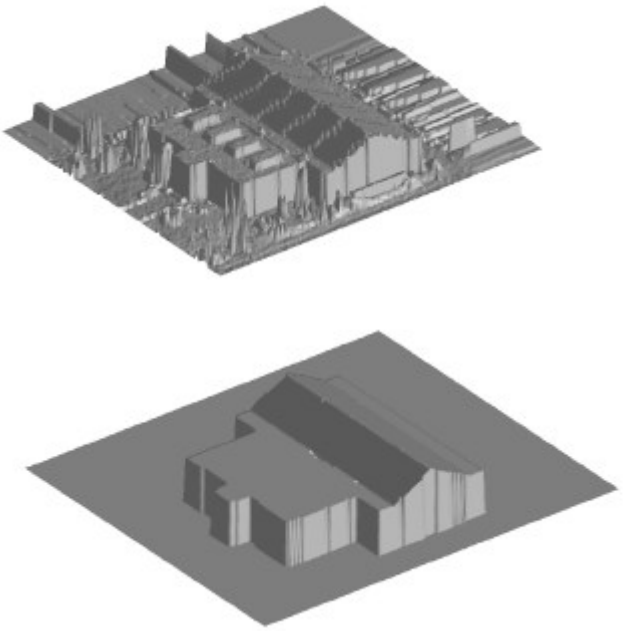

Figure 5. The Original and Refined DEM (Building 1)

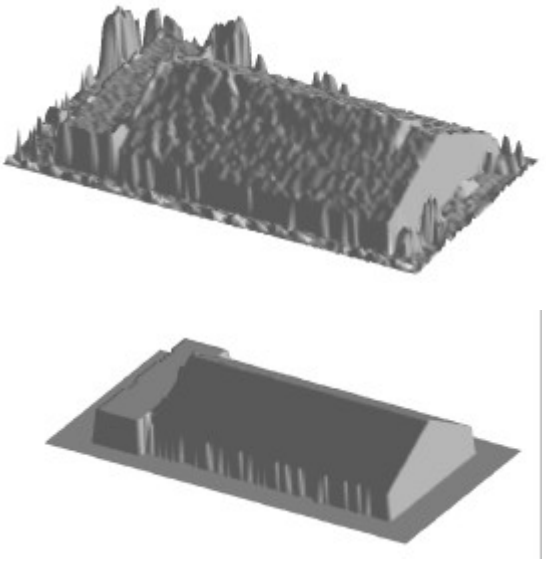

Figure 6. The Original and Refined DEM for Building 2

5. ROOF BORDERS EXTRACTION

The roof region borders are extracted after finding the roof regions. Roof border points are points that have at least one point of its 8-connected neighbors not from the same region (Rosenfeld and Kak, 1982). Figure 7-a and b show the extracted roof region borders.

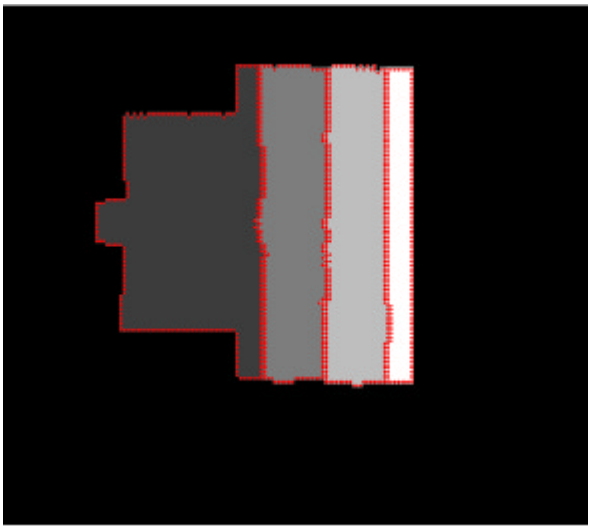

Figure 7-a. Border Points (Building 1)

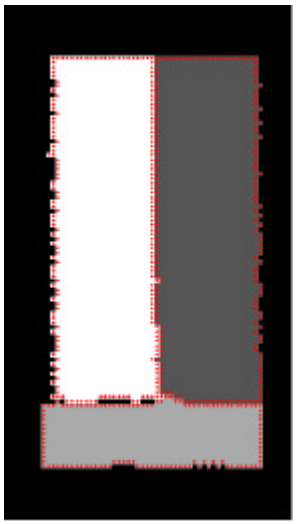

Figure 7-b. Border Points (Building 2)

In order to convert the extracted roof border points into polygons we used the algorithm presented in Bimal and Kumar 1991 and Bimal and Kumar (1992). The basic idea is to go through all the border points and only retain those that that are significant, i.e. those that represent vertices. The elevations of the corner points are then computed from the refined DEM. Adjacent corner points are grouped to form the building wire-frames. Figure 8 shows the two resulting building wire-frames.

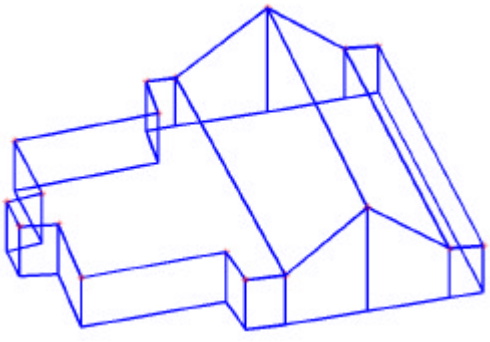

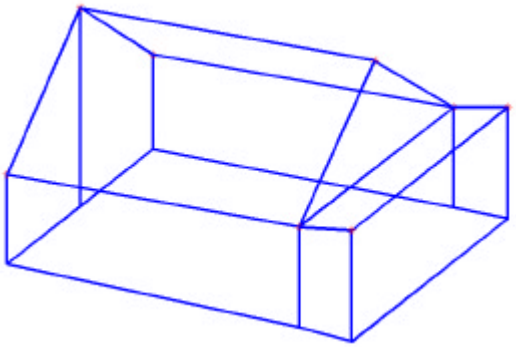

Figure 8. Building Wire-Frames

ACKNOWLEDGMENT

The authors would like to thank the Army Research Office for sponsoring this work. We also would like to thank Professor Edward Mikhail for his help and advice.

REFERENCES

Bimal R.K. and Kumar S.R. (1991). A New Approach to Polygonal Approximation. *Pattern Recognition Letters* 12, pages: 229-234.

Bimal R.K. and Kumar S.R. (1992). An Algorithm for Polygonal Approximation of Digitized Curves. *Pattern Recognition Letters 13*, pages: 489-496.

Davies *et. al.* (1988) Davies E.R., Dphil M.A., Phys C., and Flnst P. (Jan. 1988). Application of the Generalized Hough Transformation to Corner Detection. *IEEE Proceeding*, Vol. 135, Pt. E, No. 1.
Jain A.K. (1989). *Fundamentals of Digital Image Processing*. Prentice Hall, Inc., Englewood Cliffs, NJ 07632.

Jennifer L. and Jeff W. (1999). Scanning laser mapping of the coastal zone: the SHOALS system. *ISPRS Journal of Photogrammetry & Remote Sensing*, Vol. 54, pages: 123–129.

Marshall J. (1998). *Gross Error Detection in Survey Networks by L1 Norm Minimization*. Ph.D. Purdue University.

Mikhail *et. al*. (2001) Mikhail E.M., Bethel J., and McGlone J. (2001). *Introduction to Modern Photogrammetry.* Join Wiley & Sons. Inc., New York.

Morgan M. and Tempeli K. (2000). Automatic Building Extraction from Airborne Laser Scanning Data. *Proceeding of the 19th ISPRS Congress*, Book 3B, pages: 616-623, Amsterdam.

Renslow M. (2001). Development of a Bare Ground DEM and Canopy Layer in NW Forestlands Using High Performance LIDAR. *ESRI international user conference.*

Rosenfeld A. and Kak A.C. (1982): *Digital Picture Processing*. Academic Press. Inc., 2nd edition.

Seresht M. and Azizi A. (2000). Automatic Building Recognition from Digital Aerial Images. *Proceeding of the 19th ISPRS Congress*, Book 3B, pages: 792-798, Amsterdam.

Wang Z. (2000). Building Extraction and Reconstruction from LIDAR Data. *Proceeding of the 19th ISPRS Congress*, Book 3B, pages: 958-964, Amsterdam.

Wehr A. and Lohr U. (1999). Airborne Laser Scanning - An Introduction and Overview. *ISPRS Journal of Photogrammetry & Remote Sensing*, Vol. 54, pages: 68-82.

Zhao B. and Trinder J. (2000). Integrated Approach Based Automatic Building Extraction. *Proceeding of the 19th ISPRS Congress*, Book 3B, pages: 1026-1032, Amsterdam.